

論文 Numerical Analysis of the Size Effect in Pull-out Tests

Ahmed Saad Eldin MORGAN*¹, Junichiro NIWA*², and Tada-aki TANABE*³

ABSTRACT: This paper discusses the size effect with respect to the pull-out failure of headed anchor embedded in concrete. One of the goals of this research is to apply the nonlinear fracture mechanics to design problems encountered by the engineering society. In this investigation a newly developed model based on fictitious crack approach with two orthogonal rod elements was employed. In the following, the numerical investigations to describe the behavior of headed anchor under tension loading will be presented. However, the behavior of the anchor with a concrete cone failure, in particular the crack propagation in the concrete, as observed in numerical analysis, will be explained.

KEY WORDS: concrete fracture, size effect, finite element, discrete model, fictitious crack, rod elements, pull-out tests, headed anchors

1. INTRODUCTION

The fastening is a rapidly developing technology in the concrete industry. At present, the design of fastenings is mainly based on empirical equations. In order to get a better understanding of the anchor behavior, fracture mechanics must be used. However, due to the complicated fracture process (mixed mode crack propagation) only few theoretical investigations are available [1]. Therefore, numerical studies were performed to investigate the behavior of headed anchors embedded in a large concrete blocks.

The problem is physically three dimensional but mathematically two dimensional, because the solid of revolution can be considered axially symmetric if its geometry and material properties are independent of the circumferential coordinate θ .

This paper represents an energetic model of the fracture behavior of concrete where the failure cone is simulated by a discrete crack sewed by two orthogonal rod elements. By incorporating arc-length method, the post peak behavior can be captured even for snap-back instability. Application of this model for calculating the ultimate strength of headed anchor is compared with CEB empirical equation [2]. The comparison with experiments is not presented. However, such a comparison can be certainly done for the small embedded depths with small concrete blocks, but for the large embedded depths with large concrete blocks, it is very difficult to perform the experiments.

2. THE PROGRAM

Bodies of revolution have a nodal circles, not nodal points for axisymmetric problem subjected to axisymmetric boundary or restriction conditions, the material points have only u (radial), and w (axial) displacement components. The analytical procedure is essentially equivalent to that of plane stress, so a program based on the plane quadratic elements can be used. Essential changes consist of adding more terms to the [B] and [D] matrices.

For concrete finite elements around the crack path it was considered as elastic in tension. The

*1 Department of civil engineering, Nagoya University, Member of JCI

*2 School of civil engineering, Asian Institute of Technology, Dr., Member of JCI

*3 Department of civil engineering, Nagoya University, Prof., Member of JCI

results of the deformation measurements and visual crack observations lead to the conclusion that the nonlinear behavior of the concrete is concentrated in a discrete crack [3] or a crack band with small width [4].

Concrete elements in compression is modeled by bilinear stress-strain curve as shown in Fig.1.

3. FICTITIOUS CRACK SIMULATION OF THE CONCRETE FAILURE CONE

Two orthogonal rod elements (Fig.2) are used to simulate the crack and represent the localized crack zone. The rod element perpendicular to crack exhibits nonlinear stress-strain behavior of concrete modeled by the 1/4th softening curve (Fig.3). For this concrete, the fracture energy remains constant and is equal to 100 (N/m) as recommended by many researches [1]. The length of the rod element is assumed as unity ($L=1$). The stiffness matrix of the rod element perpendicular to the crack path is given using the force-displacement relation in the global system of axes as follows:

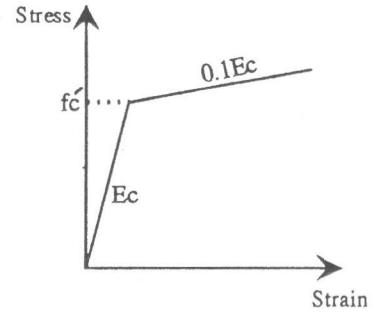


Fig.1 Concrete model in compression

$$\begin{bmatrix} F_x^i \\ F_y^i \\ F_x^j \\ F_y^j \end{bmatrix} = \frac{A_c E^*}{L} \begin{bmatrix} \cos^2 \theta & \sin \theta \cos \theta & -\cos^2 \theta & -\sin \theta \cos \theta \\ & \sin^2 \theta & -\sin \theta \cos \theta & -\sin^2 \theta \\ \text{Symmetry} & & \cos^2 \theta & \sin \theta \cos \theta \\ & & & \sin^2 \theta \end{bmatrix} \begin{bmatrix} u^i \\ v^i \\ u^j \\ v^j \end{bmatrix} \quad (1)$$

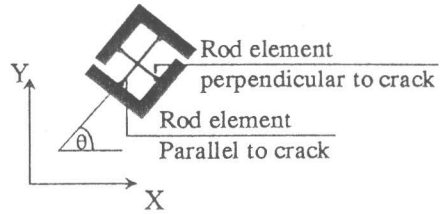


Fig.2 The rod elements for crack simulation

where A_c is the area of concrete served by this rod element, and E^* is the value of the elasticity modulus of concrete as defined later by Eq.(4) and Eq.(6).

Using the 1/4th model curve (Fig.3), the strain can be calculated which is equivalent to the crack width and then the corresponding stress can be obtained. Also, the compression bilinear curve is incorporated to the 1/4th tension softening model to simulate the rod element under compression as shown in Fig.3.

For the 1/4th tension softening model,

$$\varepsilon_p = \frac{f_t}{E_c} \quad \varepsilon_1 = 0.75 \frac{G_F}{f_t L} \quad \varepsilon_2 = 5 \frac{G_F}{f_t L} \quad (2)$$

$$\sigma = \begin{cases} E_c \varepsilon & 0 < \varepsilon \leq \varepsilon_p \\ f_t - \frac{0.75 f_t (\varepsilon - \varepsilon_p)}{\varepsilon_1 - \varepsilon_p} & \varepsilon_p < \varepsilon \leq \varepsilon_1 \\ \frac{f_t}{4} - \frac{f_t (\varepsilon - \varepsilon_1)}{4(\varepsilon_2 - \varepsilon_1)} & \varepsilon_1 < \varepsilon \leq \varepsilon_2 \\ 0 & \varepsilon_2 < \varepsilon \end{cases} \quad (3)$$

$$E_R = \begin{cases} E_c & 0 < \varepsilon \leq \varepsilon_p \\ E_{\text{Secant}} & \varepsilon_p < \varepsilon \leq \varepsilon_2 \\ 0.00001 E_c & \varepsilon_2 < \varepsilon \end{cases} \quad (4)$$

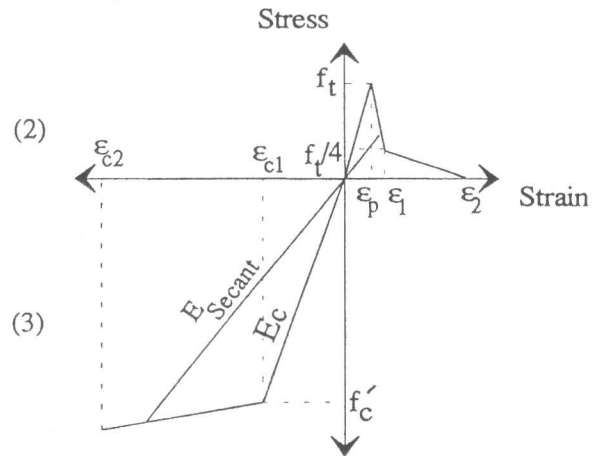


Fig.3 Stress-strain model for perpendicular rod element

For the compression model,

$$\sigma_{comp.} = \begin{cases} E_C |\epsilon_{c1}| & 0 < |\epsilon| \leq |\epsilon_{c1}| \\ f'_c + 0.1E_C \left(\frac{|\epsilon| - |\epsilon_{c1}|}{|\epsilon_{c2}| - |\epsilon_{c1}|} \right) & |\epsilon_{c1}| < |\epsilon| \leq |\epsilon_{c2}| \\ 0 & |\epsilon_{c2}| < |\epsilon| \end{cases} \quad (5)$$

$$E_{comp.} = \begin{cases} E_C & 0 < |\epsilon| \leq |\epsilon_{c1}| \\ E_{secant} & |\epsilon_{c1}| < |\epsilon| \leq |\epsilon_{c2}| \\ 0.00001E_C & |\epsilon_{c2}| < |\epsilon| \end{cases} \quad (6)$$

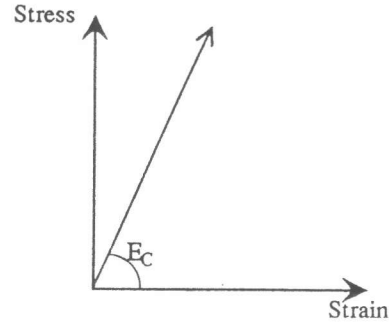


Fig.4 Stress-strain model for parallel rod element

where f_t and f'_c are the tensile and compressive strengths of concrete, respectively, G_F is the fracture energy of concrete, E_R is the elasticity modulus of the rod element in tension model which takes different values according to different strain stages as defined by Eq.(4). Similarly, the E_{comp} is the elasticity modulus of the rod element in compression model and its values are defined by Eq.(6), $\epsilon_{c1} = f'_c/E_C$ and ϵ_{c2} is the ultimate compressive strain of concrete which is taken to be equal to 0.0035.

Since the rod element which is parallel to the crack path is perpendicular to the other one, therefore the stiffness matrix for this rod element can be considered as $\cos(\theta+90^\circ) = -\sin\theta$, $\sin(\theta+90^\circ) = \cos\theta$ in Eq.(1). The stress-strain relation for the parallel rod element is taken as linear elastic till the tensile stress in the perpendicular rod element exceeds the tensile strength of concrete (Fig.4). Thus, when the crack starts at a certain perpendicular rod element, the resistance of corresponding parallel rod element vanishes.

4. NUMERICAL SOLUTION TECHNIQUE FOR NONLINEAR ANALYSIS

The current analysis is tried to trace the entire load-deformation response of the concrete structures. However, tracing of limit point and post limit path is notoriously difficult especially for structures which have a response involving a snap back behavior. However, it is important to know whether the structure collapse is of a ductile or brittle form, and to define a material modeling including the softening behavior. The arc-length procedure [5] was established for dealing with overcoming limit points in a nonlinear solution path. Moreover, a technique has been adopted [6] to maintain the symmetric banded nature of the equilibrium equations.

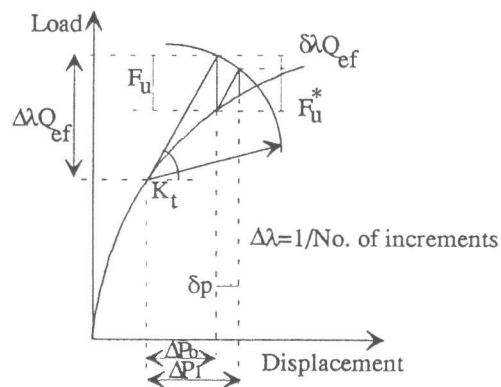


Fig.5 The spherical arc-length procedure

The basic idea in all arc-length methods is to modify the load level at each iteration, rather than holding the applied load level constant during a load step, so that the solution follows some specified path until convergence is attained.

5. THE RESULTS OF AXISYMMETRIC PULL-OUT ANALYSIS

The geometry of a concrete cylindrical block is illustrated in Fig.6. Six different embedded depths are considered, such as $d=50.0, 150.0, 450.0, 600.0, 1000.0$, and 2000.0 mm. The concrete properties are identical for all six concrete blocks: $f'_c=30.0$ MPa, $f_t=3.0$ MPa, $G_F=100$ N/m, and $E_C=30.0$ GPa.

The finite element model used for the pull-out analysis is given in Fig.6. The mesh consists of 268 elements including 8,7, and 6 noded quadrilateral elements. Also, 6 noded triangular element was utilized along the crack path. Further, it is noticed that the numerical instabilities through the calculations are reduced as much as the rod elements were used along the crack path. Thus, the 6 noded triangular element was used, to provide 21 perpendicular rod elements along the failure cone surface. The number of nodes in this mesh was 858.

The shaft of the bolt has not been modeled because the shaft has been assumed to be unbonded with the concrete. The geometrical dimensions of the analyzed specimens were determined according to the RILEM Round Robin Analysis requirements of Anchor Bolts [1]. Also, the experimental observation showed that the influence of the volume below the bolt head should be taken large to avoid breaking the concrete blocks into 4 pieces instead of producing the concrete failure cone [1]. The perfect bond between steel and concrete was assumed on the upper edge of the anchor head only [1].

Based on extensive parametric study the inclination of the diagonal failure surface was determined. The diagonal shear crack was oriented at angles ranges between 26° and 76° , then 11 finite element meshes were rearranged with respect to the chosen path to cover precisely all possibilities of crack inclinations. The chosen embedded depth for performing these strength minimization calculations is 50mm. However, it was found that the inclination of 60° gives the minimum pull-out strength (Fig.7), therefore this angle was selected for further calculations. The failure cone surface was assumed as a discrete crack from the outer anchor head edge to the top surface of the concrete block at the inner reaction ring location (Fig.6). In the present paper the fictitious crack was propagated from the anchor head edge at distance $0.1d$ from the axis of symmetry, which was taken as a standard practice in RILEM report [1]. The analysis was done by the arc-length procedure and was stable in all cases in the whole softening range.

Fig.8 shows the tendency of the nominal pull-out strength to decrease with the increase in the embedded depth. This behavior is known as the size effect. Also, as shown in Fig.8 the size effect disappears for large embedded depths, and the nominal pull-out strength of the concrete blocks

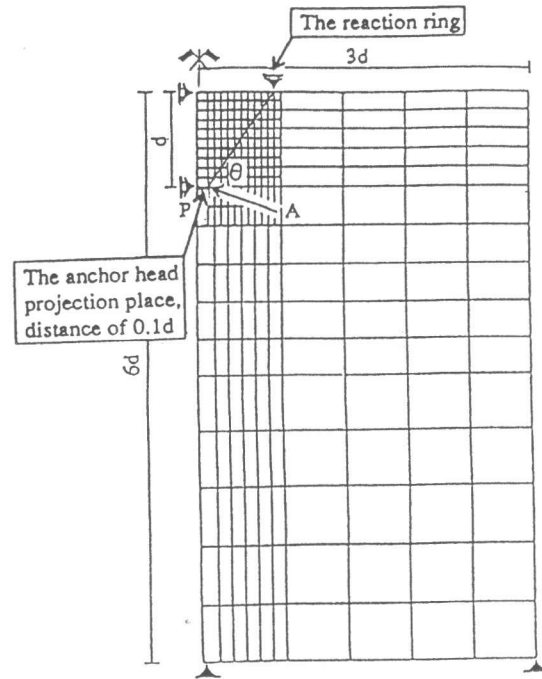


Fig.6 The mesh for the concrete block

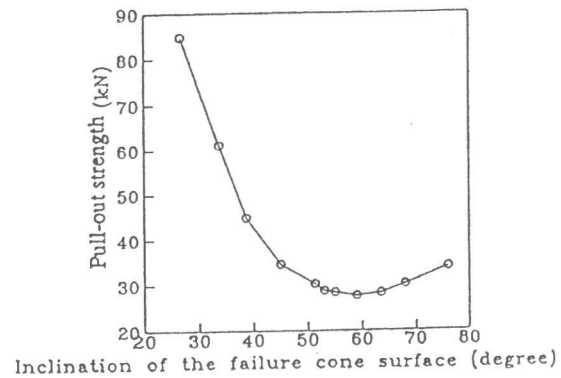


Fig.7 Variation of ultimate pull-out force with the cone failure surface inclination θ

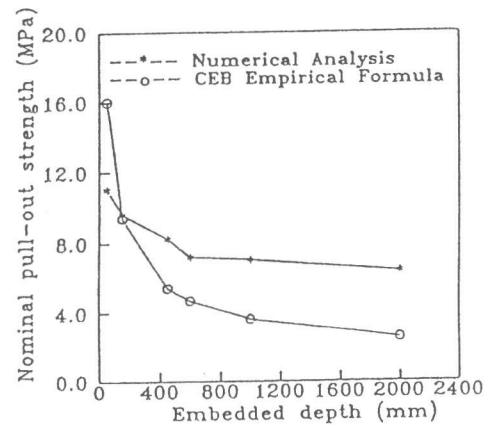


Fig.8 Comparison between the nominal pull-out strength from the numerical analysis and the CEB empirical formula Eq.(8)

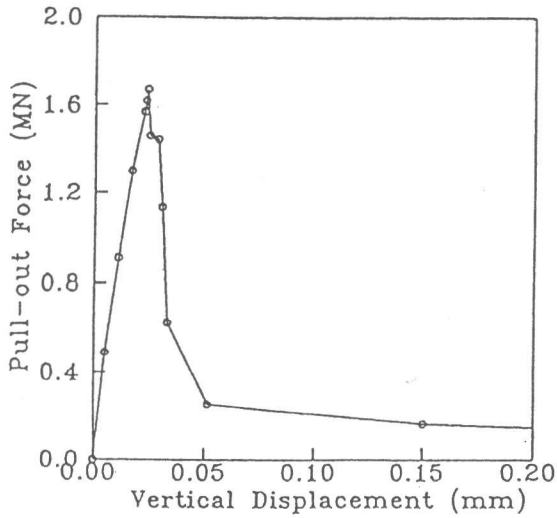


Fig.9 Pull-out force versus displacement diagram for embedded depth 450mm

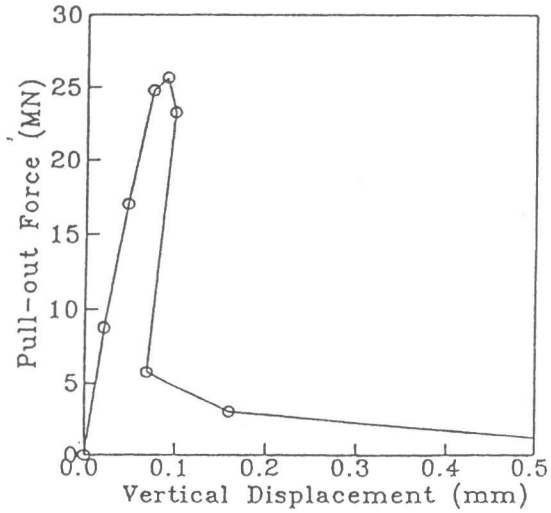


Fig.10 Pull-out force versus displacement diagram for embedded depth 2000mm

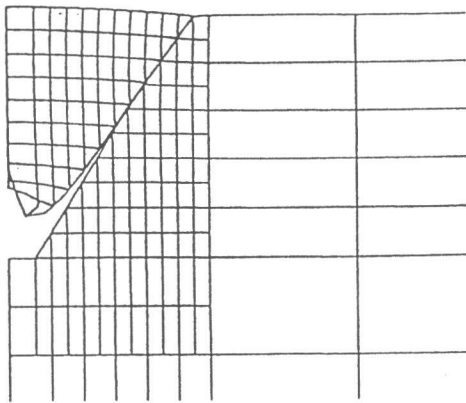


Fig.11 Deformed shape at the peak load

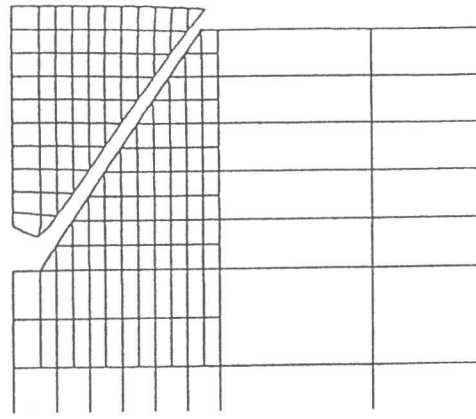


Fig.12 Deformed shape for the second increment after the peak load

tends to be bounded with a certain limit. The nominal pull-out strength in Fig.8 is calculated by devising the ultimate pull-out strength by the square of the embedded depth as illustrated in Eq.(7).

$$\sigma = N_u / d^2 \quad (7)$$

where σ is the nominal pull-out strength, N_u is the ultimate pull-out strength, and d is the embedded depth.

Also, the results of this study with the CEB empirical formula are illustrated in Fig.8.

The CEB equation that gives the relation between the induced ultimate pull-out strength N_u and the embedded length h_{ef} is as follows:

$$N_u = 2.1(E G_F)^{0.5} h_{ef}^{1.5} \quad (8)$$

where: E is the Young's modulus of concrete, G_F is the fracture energy of concrete and h_{ef} is the embedded depth of the anchor from the top surface of concrete to the top surface of the anchor head.

Figs.9,10 show the pull-out force vs. displacement diagrams of embedded depths 450mm and 2000mm, respectively. For small embedded depth such as 450mm, the pull-out force vs. displacement

diagram (Fig.9) is stable in all load levels before and after the peak. Moreover, Fig.9 shows that the failure is ductile and the snap back phenomenon will not occur for such small embedded depths.

Fig.10 shows that the pull-out force vs. displacement diagram for large embedded depth such as 2000mm, and it exhibits a post peak snap back response, which reflects the brittle behavior of such large embedded depths. It can be concluded that the pull-out behavior of headed anchors is significantly affected by the embedded depths, and consequently the concrete block size, and the failure changes from ductile to brittle as the embedded depth, and consequently the associated concrete block increases. Also, it is better to mention that the detected point for examining the vertical upward displacements in Figs.9,10 is the outer end of the anchor head (point A shown in Fig.6). The snap back phenomenon occurs because there is a sudden bifurcation process which leads to a sudden drop in both load and deflection. In other words, fracture of concrete leads to brittle failures and as a result causes the size effect of decreasing strength in structures of increased sizes.

Furthermore, Figs.11,12 show the deformed shapes at the peak load and at the next second increment after the peak in the case of embedded depth 2000mm. It can be noticed that the displacements at the outer end of the anchor head in Fig.12 is smaller than that of Fig.11, which illustrates the effect of snap back phenomenon.

6. CONCLUSIONS

It is possible to study the influence of different variables on pull-out strength of headed anchor embedded in concrete blocks analytically by means of nonlinear fracture mechanics. In particular, fracture mechanics offers a possibility to explain the size effect in pull-out strength. It was observed that for small embedded depth the nominal pull-out strength of headed anchors embedded in concrete blocks is profoundly affected by the size effect. On the other hand, for large headed anchors embedded in large concrete blocks, the numerical predictions showed that the size effect becomes negligible. Moreover, the snap back phenomenon occurs when the embedded depth, and consequently the associated concrete block size increases, and the brittle behavior of concrete blocks becomes significant. Also, it is found that the inclination of failure cone surface with 60° gives the minimum pull-out strength, which indicates that the commonly adapted method assuming 45° failure surface yields exaggerated resisting load.

REFERENCES

- 1) RILEM TC 90-FMA : Fracture Mechanics of Concrete - Applications, Round Robin Analysis of Anchor Bolts, Preliminary Report, 2nd ed., May 1991.
- 2) CEB COMITE EURO-INTERNATIONAL DU BETON : Fastenings to Reinforced Concrete and Masonry Structures, State-of-the-art report, No. 206,207, August 1991.
- 3) Hillerborg, A., Modeer, M. and Peterson, P.E., "Analysis of Crack Formation and Crack Growth in Concrete by Means of Fracture Mechanics and Finite Element," Cement and Concrete Research. Vol. 6, 1976, pp. 773-782.
- 4) Bazant, Z.P. and Oh, B.H., "Crack Band Theory for Fracture of Concrete," Mater. and struct., Vol. 16, No. 93, 1983, pp. 155-177.
- 5) Riks, E., "An Incremental Approach to the Solution of Snapping and Buckling Problems," Int. J. Solids Struct., Vol. 15, 1979, pp. 524-551.
- 6) Batoz, J.L. and Dhatt, G., "Incremental Displacement Algorithms for Nonlinear Problems," Int. J. Num. Meth. Engng Vol. 14, 1979, pp. 1262-1266.